Ferromagnetic resonance in as-deposited and annealed Fe-SiO_2 heterogeneous thin films

A. Butera*
Centro Atómico Bariloche and Comisión Nacional de Energía Atómica, 8400 San Carlos de Bariloche, Río Negro, Argentina

J. N. Zhou and J. A. Barnard
Center for Materials for Information Technology and Department of Metallurgical and Materials Engineering, The University of Alabama, Tuscaloosa, Alabama 35487-0209

(Received 5 March 1999; revised manuscript received 17 May 1999)

The magnetic properties of sputtered Fe-SiO_2 composite thin films, containing an Fe volume fraction ranging from 0.42 to 0.90, have been characterized by means of ferromagnetic resonance. Experiments at *X*-band ($\nu = 9.4$ GHz) and *Q*-band frequencies ($\nu = 35.4$ GHz) were done on as-deposited and annealed (2 h, 435 °C) samples as a function of the Fe concentration. In general only one line corresponding to the uniform precession mode is observed. However, when the external field is applied perpendicular to the film plane one or two extra lines are observed at lower fields. More interestingly, when the concentration is very close to the percolation threshold for the Fe granules ($f_p \sim 0.62$), more than 15 equally spaced lines are found. The origin of these additional resonances does not seem to be related to the film thickness, as usually happens with standing spin waves in continuous films, but to the divergence of the correlation length at the percolation concentration. It was found that the effective anisotropy field H_{eff}, which takes into account demagnetization and anisotropy fields, decreases almost linearly as the Fe fraction is reduced up to f_p, where a sudden decrease is observed. The resonance linewidth and the calculated *g* value also have distinctive features near the percolation threshold. Sample annealing produced a broader distribution of particle sizes and shapes that reflects in a resonance linewidth 3–6 times larger than for similar as-deposited samples. All these effects are closely related to the intricate geometry of the Fe granules near the percolation concentration.
[S0163-1829(99)01338-7]

I. INTRODUCTION

Heterogeneous, composite, or simply ''granular'' materials consist of very small metal granules embedded in an immiscible matrix. Their unique nanostructure and the relative simplicity of changing the particle size and concentration make these systems almost ideal for investigations of the physical properties of nanostructured materials. In the last few years extensive research has been made in granular magnetic thin films with potential applications in the magnetic recording industry. The ferromagnetic (FM)/metallic immiscible alloys, exhibiting giant magnetoresistance, are of interest as magnetic sensors and read heads.[1] FM/insulating nanocomposites have been proposed as promising high coercivity, low noise, magnetic recording media.[2] Chien and co-workers[3] studied in detail the magnetic properties of FM composites. They found that if the volume fraction f of the FM metal is below the percolation threshold f_p (defined as the volume concentration where a continuous network of connecting granules appear), the granules are single domain and usually exhibit hard magnetic properties (eventually affected by superparamagnetic effects, especially for very small grains). When f is larger than f_p the FM material surrounds the insulator forming a networklike structure. The relatively soft magnetic behavior of a continuous FM film is then recovered. Room-temperature coercivity in the Fe-SiO_2 system has a maximum for $f \sim f_p \sim 0.55$ in thick films.[4] For films thinner than 40 nm it was observed that the percolation threshold is strongly dependent on the annealing conditions and the film thickness.[5] As-deposited films percolate at $f_p \sim 0.62$ for all thickness below 40 nm. Annealed films, on the other hand, show an increasing percolation concentration when the film thickness is reduced ($f_p \sim 0.44$ for 40 nm to $f_p \sim 0.78$ for 5 nm). Transmission electron microscopy (TEM) studies have revealed the crucial role played by the intricate geometrical nanostructure on the magnetic properties.[3] Coercivities exceeding 1000 Oe have been observed in optimally annealed samples near f_p. The origin of this very large coercivity (that can exceed 3000 Oe at 5 K) is still unclear. It was suggested that a very large effective anisotropy constant that includes the contribution of magnetocrystalline anisotropy and ''other'' sources is responsible for the observed behavior.[3] The fact that the maximum coercivity is observed at the percolation concentration, where the shape of the FM clusters changes dramatically from equiaxed to ''wormylike,'' is a good indication of the importance of shape anisotropy.

Ferromagnetic resonance (FMR) has proved to be a very useful tool in the characterization of magnetic films. Through the analysis of the spectra obtained from the excitation of uniform precession or excited modes, valuable information on the effective fields, particle shape and size distribution, ferromagnetic exchange constant, etc., can be obtained or deduced.

In this work we will present the FMR results obtained in a series of Fe-SiO_2 granular films. The paper is organized as follows: the sample preparation and the experiments performed are explained in Sec. II. The analysis of the results

obtained from the uniform mode and the additional resonances are discussed in Secs. III A through III C. Conclusions are presented in Sec. IV.

II. SAMPLE PREPARATION AND EXPERIMENTS

Granular Fe-SiO_2 films were prepared by rf magnetron sputtering. The top part of a 20 cm SiO_2 target was covered with a semicircular high-purity Fe foil to obtain a nearly linear composition gradient in the vertical direction ($\sim$0.45 %/mm). The Fe composition ranges from $f=0.42$ to $f=0.90$ Fe volume fraction. Films used in this study were deposited on eight 18 mm$\times$18 mm Fisher finest premium cover glass disposed in a single vertical column. The film thickness obtained with this geometry is not uniform and changed in an approximately parabolic way from $\sim$24 nm at the central substrate to $\sim$16 nm 76 mm above or below the center. All necessary corrections due to this thickness variation have been made in the film volume calculations. After sputtering the films, 48 samples of 3 mm$\times$3 mm were cut from the original slides covering a total vertical lenght of 144 mm. This sample size assures a composition variation smaller than $f=0.015$ and a thickness change $<$0.4 nm in each sample. Some selected samples have been annealed for 2 h at 435°C in a closed chamber with flowing pure Ar at a pressure of 10^{-2} Torr. It is worth mentioning that all samples have been covered with a 70 nm protective SiO_2 layer to prevent oxidation. A very detailed explanation of the sample preparation and the microstructural characterization can be found in Ref. 5.

Feromagnetic resonance measurements have been done on a Bruker ESP 300 system at *X*-band (ν=9.4 GHz) and *Q*-band frequencies (ν=35.4 GHz) at room temperature. A standard field modulation technique was used so that the detected signal corresponded to the derivative of the absorbed microwave power. Samples were mounted at the cavity center with the film plane parallel to the radio frequency (rf) field and the dc field changing from the in-plane to the out-of-plane direction. To study the existence of in-plane anisotropy the dc magnetic field was also varied in the film plane. Very small samples (less than 1 mm$\times$1 mm), obtained from the previously cut 3 mm$\times$3 mm samples, were used to prevent excessive loading of the cavity.

III. EXPERIMENTAL RESULTS AND DISCUSSION

A. Uniform mode

1. Normal modes

The FMR spectrum for H applied parallel to the film plane consists of a single absorption line located at a field lower than that corresponding to $g=2$. If the sample is rotated with respect to H, the resonance field increases and reaches a maximum when H is perpendicular to the film. To explain this behavior the following simple expression for the magnetic free energy may be used:

$$F=\frac{1}{2}\mathbf{M}_0\cdot\underline{\mathbf{N}}\cdot\mathbf{M}_0+\frac{K_z}{M_0^2}(\mathbf{M}_0\cdot\hat{z})^2-\mathbf{M}_0\cdot\mathbf{H}, \qquad (1)$$

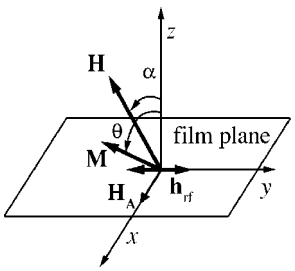

FIG. 1. Relative orientation of the magnetization vector, the applied field and the radio-frequency field with respect to the film plane. H_A indicates the direction of a very small in-plane anisotropy (observed only for $f\gtrsim 0.7$) coincident with the composition gradient.

where $\mathbf{H}$ is the applied field external field and $\mathbf{M}_0$ is the saturation magnetization. The first term represents the demagnetization energy ($\underline{\mathbf{N}}$ is the diagonal demagnetization tensor), the second term comes from either an easy plane ($K_z>0$) or easy axis ($K_z<0$) ''intrinsic'' anisotropy, that includes all contributions (magnetocrystalline, stress, interface) but shape anisotropy, and the last term is the Zeeman energy. The relative position of the film with respect to the axis and vectors is sketched in Fig. 1.

Obtaining the resonance condition for the uniform mode from Eq. (1) requires one to solve the damped Landau-Lifshitz (LL) equation of motion,[6,7]

$$\frac{1}{\gamma}\frac{\partial\mathbf{M}}{\partial t}=-\mathbf{M}\times\mathbf{H}_i-\frac{\lambda}{\gamma M^2}\mathbf{M}\times[\mathbf{M}\times\mathbf{H}_i]. \qquad (2)$$

The gyromagnetic ratio of the precessing moments γ is related to the g factor by $\gamma=-g\mu_\beta/\hbar$ (μ_β is the Bohr magneton, $\hbar$ is the Plank constant). Different experimental values of the g factor at room temperature for bulk FM Fe can be found in the literature: $g=2.12-2.17$,[8] $g=2.10$.[9] The general accepted value for thin films is $g=2.09$,[10] although in granular Fe-SiO_2 smaller values ($g=1.91-2.07$) have been reported.[11–13] The internal magnetic field $\mathbf{H}_i$ and the free energy F are related through the simple relationship $\mathbf{H}_i=-\partial F/\partial\mathbf{M}$.[14] The magnetization is divided into a time-independent and a time-dependent part: $\mathbf{M}(t)=\mathbf{M}_0+\mathbf{m}(t)$. The temporal dependence of $\mathbf{m}(t)$ is chosen to be of the form $\mathbf{m}(t)=\mathbf{m}_0e^{iwt}$. The second term on the right of Eq. (2) is the LL phenomenological damping that accounts for the overall intrinsic contribution to the loss. The relaxation is characterized through the parameter λ.

Using Eqs. (1) and (2), the condition $\partial\mathbf{M}_0/\partial t=0$, and discarding terms of the form $\mathbf{m}\times\mathbf{m}$, a set of linear equations in m_x, m_y, and m_z, is obtained. Solving these equations it is possible to arrive to the following expression for the normal modes (the damping term is omitted for the moment):

$$\left(\frac{\omega}{\gamma}\right)^2=(H\cos\alpha-H_{\text{eff}}\cos\theta)^2+H\sin\alpha(H\sin\alpha+H_{\text{eff}}\sin\theta), \qquad (3)$$

the effective anisotropy field is defined as

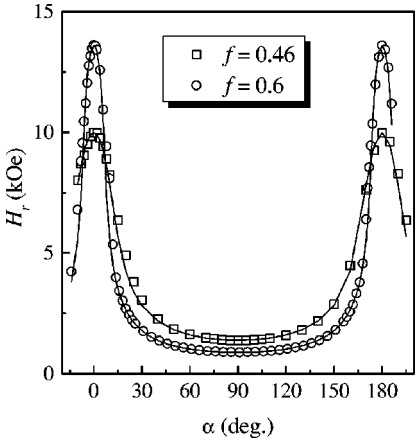

FIG. 2. Angular variation of the X-band ($\nu = 9.4$ GHz) resonance field as a function of the angle α formed between the applied external field and the film normal for $f = 0.46$ and $f = 0.6$. The continuous lines are the fits obtained after solving Eqs. (3) and (5) with the following parameters: $g = 2.01$, $H_{\text{eff}} = 6645$ Oe, for $f = 0.46$ and $g = 2.11$, $H_{\text{eff}} = 10430$ Oe, for $f = 0.60$.

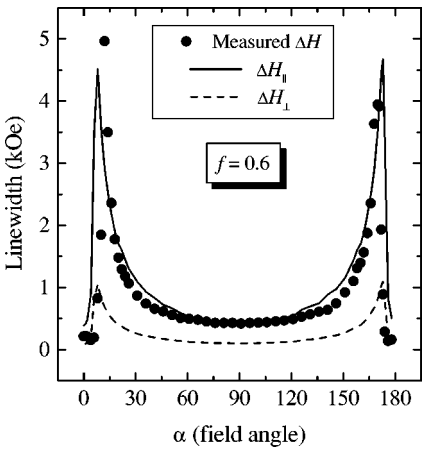

FIG. 3. Angular variation of the X-band ($\nu = 9.4$ GHz) linewidth as a function of the angle α formed between the applied external field and the film normal for $f = 0.6$. The two fits have been obtained using Eqs. (7) and (8) and $H_{\parallel} = 887$ Oe, $\Delta H_{\parallel} = 417$ Oe, $H_{\perp} = 13602$ Oe, and $\Delta H_{\perp} = 100$ Oe.

$$H_{\text{eff}} = \frac{2K_z}{M_0} + (N_{\perp} - N_{\parallel})M_0, \tag{4}$$

where $N_{\perp}$ and $N_{\parallel}$ are the demagnetization factors perpendicular and parallel to the film plane (both in-plane demagnetization factors are assumed to be the same). It is importantant to mention that in very thin continuous ferromagnetic films $N_{\parallel}$ can be usually taken as zero. However, in granular films it was found that the shape of the individual grains is important when describing the overall magnetic behavior (see, for example, Refs. 15 and 16).

The out-of-plane angle θ is related to α by the equilibrium condition:

$$H \sin(\theta - \alpha) = \frac{H_{\text{eff}}}{2} \sin 2\theta. \tag{5}$$

Isotropic in-plane magnetization was assumed to simplify the mathematics, thus the in-plane magnetization angle φ was set to zero. It should be mentioned that for $f > 0.7$ there is a very small in-plane anisotropy[5] that does not affect the general results as will be discussed in Sec. III B 5. Equations (3) and (5) reduce to the well-known Kittel expressions when $\alpha = 0$ ($H\perp$ film plane), and $\alpha = \pi/2$ ($H\parallel$ film plane),[17]

$$\left(\frac{\omega}{\gamma}\right)^2 = (H - H_{\text{eff}})^2 \quad \alpha = 0, \tag{6a}$$

$$\left(\frac{\omega}{\gamma}\right)^2 = H(H + H_{\text{eff}}) \quad \alpha = \pi/2. \tag{6b}$$

Note that both Eqs. (3) and (5) and Eq. (6) depend on a single physical parameter which represents the effective anisotropy energy. The angular variation of the resonance field H_r of two selected films ($f = 0.46$ and $f = 0.60$) is shown in Fig. 2. The continuous lines are the best fits obtained by numerical resolution of Eqs. (3) and (5). As mentioned before the resonance field is below the field corresponding to $g = 2.09$ and changes very little when H is applied close to the film plane. If H is moved out to the perpendicular direction a sharp increase in H_r is observed approximately 30 degrees apart from the film normal. Note that the difference between the resonance fields in the parallel and perpendicular orientations is larger for higher Fe concentrations implying [see Eq. (6)] a larger effective anisotropy field for higher Fe concentrations. This behavior will be discussed in more detail in the next section.

2. Linewidth

The angular variation of the linewidth ΔH of the $f = 0.6$ film is presented in Fig. 3. The minimum is found for $\alpha = 0$, and there is also a relative minimum for $\alpha = \pi/2$. Around $\alpha = 12°$ the linewidth has a maximum of ~4–5 kOe. The exact determination of ΔH near the maximum is quite difficult because the line shape is strongly deformed, thus the given values may be affected by large errors. If the relaxation term is now considered in Eq. (2) an expression for the frequency linewidth can be obtained:[7]

$$\frac{\Delta\omega}{\gamma} = \frac{\lambda}{\gamma M_0}[2H\cos(\alpha - \theta) - H_{\text{eff}}(3\cos^2\theta - 1)]. \tag{7}$$

The field linewidth ΔH is related to $\Delta\omega/\gamma$ through the relation[18]

$$\Delta H \approx \left.\frac{\partial H}{\partial(\omega/\gamma)}\right|_{H_r} \frac{\Delta\omega}{\gamma} + \left.\frac{\partial H}{\partial\theta}\right|_{H_r} \Delta\theta. \tag{8}$$

The first term is a first-order approximation that is valid only when the condition $\Delta\omega/\omega \ll 1$ holds. The derivative $\partial H/\partial(\omega/\gamma)$ is normally close to one for large microwave frequencies (where the resonance fields are usually large) and for isotropic samples. For intermediate frequencies (for example, X band) the magnetic resonance occurs at fields where the magnetization vector may not be aligned with the magnetic field. During a standard FMR experiment the equilibrium angle θ changes when H is swept. The change in θ causes a variation of the resonance condition and contributes to an increase in the absorption linewidth and also a defor-

mation of the line shape. This angular effect is taken into account by the second term in Eq. (8). The angular ''width,'' $\Delta\theta$, is defined as

$$\Delta\theta=\theta\left(\frac{\omega}{\gamma}+\frac{1}{2}\frac{\Delta\omega}{\gamma},\alpha\right)-\theta\left(\frac{\omega}{\gamma}-\frac{1}{2}\frac{\Delta\omega}{\gamma},\alpha\right)$$
$$\approx\theta\left(H_r+\frac{1}{2}\frac{\Delta\omega}{\gamma}\frac{\partial H}{\partial(\omega/\gamma)}_{H_r},\alpha\right)$$
$$-\theta\left(H_r-\frac{1}{2}\frac{\Delta\omega}{\gamma}\frac{\partial H}{\partial(\omega/\gamma)}\bigg|_{H_r},\alpha\right). \quad (9)$$

Note that $\Delta\theta$ is zero when α is parallel or perpendicular to the film plane because θ is already collinear with α and the field change does not affect the orientation of **M**. For other orientations $\Delta\theta$ can be as large as 8°.

Only one free parameter $\lambda/\gamma M_0$ is available to fit the experimental data. Either the parallel ($\Delta H_\parallel$) or the perpendicular ($\Delta H_\perp$) linewidths can be used in the determination of $\lambda/\gamma M_0$. This option is advantageous in that the influence of the $\Delta\theta$ term is minimized. The results for the $f=0.6$ film, obtained by numerical resolution of Eq. (8), are shown in Fig. 3 together with the measured data. It can be seen that $\Delta H_\parallel$ gives a better fit than $\Delta H_\perp$ and even reproduces the magnitude and position of the maximum. However, it fails to predict the correct value of $\Delta H_\perp$ by a factor of 4. If $\Delta H_\perp$ is chosen, the maximum is also well predicted (although the magnitude is smaller), but again the value obtained for the 90° direction is wrong by a factor of 4. It is worth mentioning that within the theoretical framework that leads to Eq. (8), similar values of $\Delta H_\perp$ and $\Delta H_\parallel$ are predicted. The $\lambda/\gamma M_0$ values are in the range $0.02-0.06$ giving corresponding λ values of the order of 10^8 rad/s.

Up to now the only source of line broadening was assumed to come from intrinsic relaxation. It is well known that particle orientation and particle shape distributions may also be an important source of line broadening. Netzelmann[15] studied in detail the influence of particle shape, size distribution, and packing fraction in magnetic tapes. He proposed that the effective magnetostatic free energy [first term in Eq. (1)] can be approximately described by

$$F_N=\frac{1}{2}(1-f)\mathbf{M}\cdot\underline{\mathbf{N}}_p\cdot\mathbf{M}+\frac{1}{2}f\mathbf{M}\cdot\underline{\mathbf{N}}_t\cdot\mathbf{M}, \quad (10)$$

where f is the FM volume fraction (assuming complete phase separation). It is important to note that no magnetostatic interactions are assumed in this description. The effective magnetostatic energy is just a combination of the limiting cases of an isolated particle with a demagnetization tensor $\underline{\mathbf{N}}_p$ and a thin film with a corresponding factor $\underline{\mathbf{N}}_t$. Rubinstein[16] applied Netzelmann's model to explain the linewidth behavior of Co(Fe)-Cu granular alloy films. He could explain a $\Delta H_\perp$ larger than $\Delta H_\parallel$ assuming that the films could be treated as a collection of flat particles with an ellipticity parameter ε varying from $\varepsilon=0$ to $\varepsilon=\varepsilon_0$. In our case, contrary to Rubinstein's experiments, $\Delta H_\parallel$ is much larger than $\Delta H_\perp$. This means that apart from the shape, the in-plane angular distribution of particles plays an important role in the determination of the linewidths. Dubowick[19] showed that the first term in Eq. (10) must be multiplied by a factor f to correctly describe the isolated-particle to continuous-thin-film transition. The correction is especially important for loosely packed particles. Although all our films have Fe fractions larger than 0.42 we have taken into account Dubowick's correction in our calculations

Following Rubinstein's convention that the z axis is always the direction of the applied field a total demagnetization tensor can then be written as[16]

$$\underline{\mathbf{N}}=f(1-f)\underline{\mathbf{N}}_p+f\underline{\mathbf{N}}_t, \quad (11)$$

where

$$\underline{\mathbf{N}}_{t\perp}=4\pi(0,0,1) \text{ and } \underline{\mathbf{N}}_{t\parallel}=4\pi(1,0,0) \quad (12)$$

for perpendicular ($H\|\hat{z}$, film normal $\|\hat{z}$) and parallel ($H\|\hat{z}$, film normal $\|\hat{x}$) resonance, respectively, and

$$\underline{\mathbf{N}}_{p\perp}=\frac{4}{3}\pi\left[1+\frac{\varepsilon}{2}(1-3x),1-\varepsilon\left(1-\frac{3}{2}\right)x,1+\frac{\varepsilon}{2}\right], \quad (13a)$$

$$\underline{\mathbf{N}}_{p\parallel}=\frac{4}{3}\pi\left[1+\frac{\varepsilon}{2},1-\varepsilon\left(1-\frac{3}{2}\right)x,1+\frac{\varepsilon}{2}(1-3x)\right]. \quad (13b)$$

In Eq. (13) the parameter ε can range between 0 and 1 for the limiting cases of a spherical particle and an in-plane infinite cylinder, respectively. The variable x also ranges between 0 and 1 and is introduced to take into account the in-plane distribution of cylinders. In Eq. (13a) $x=0$ and $x=1$ correspond to the long axis of the cylinder parallel to the $\hat{y}$ and $\hat{x}$ directions, while in Eq. (13b) the same x values describe a cylinder parallel to $\hat{y}$ and $\hat{z}$, respectively. As we only want to show that the above model can give $\Delta H_\parallel > \Delta H_\perp$ a few simplifications will be made. First, the crystalline anisotropy term will be neglected and only the demagnetization term will be kept. Second, the intrinsic perpendicular linewidth will be assumed to be smaller than the measured one so that the extra linewidth comes from a distribution of particle ellipticities raging from $\varepsilon=0$ (spherical particles) to $\varepsilon=\varepsilon_0$. Due to the fact that the particles may be in-plane anisotropic Eq. (6) should be modified in the following way:[16]

$$\left(\frac{\omega}{\gamma}\right)^2=[H-(N_z-N_x)M_0][H-(N_z-N_y)M_0]. \quad (14)$$

The field H is replaced by the perpendicular and parallel resonance fields together with their corresponding demagnetization factors [Eq. (11)]. In the case of perpendicular resonance it can be seen that Eq. (14) is independent of x. Assuming that the linewidth comes from particles of different shapes resonating at different fields an upper limit for the linewidth is given by

$$\Delta H_\perp=H_\perp(\varepsilon=\varepsilon_0)-H_\perp(\varepsilon=0)=4\pi fM_0(1-f)\frac{\varepsilon_0}{4}$$
$$+\sqrt{\left(4\pi fM_0(1-f)\frac{\varepsilon_0}{4}\right)^2+\left(\frac{\omega}{\gamma}\right)^2}-\frac{\omega}{\gamma}. \quad (15)$$

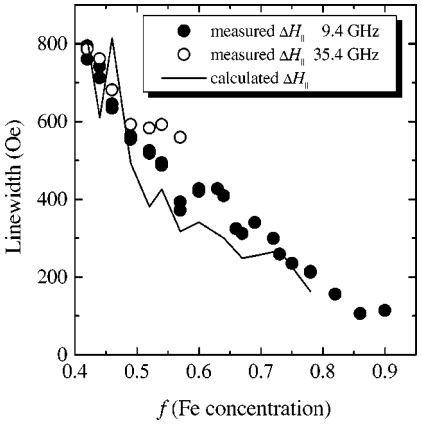

FIG. 4. Parallel linewith as a function of Fe concentration for X ($\nu=9.4$ GHz) and Q ($\nu=35.4$ GHz) bands. The continuous line corresponds to the values estimated from the measured $\Delta H_{\perp}$ and Eqs. (15) through (17).

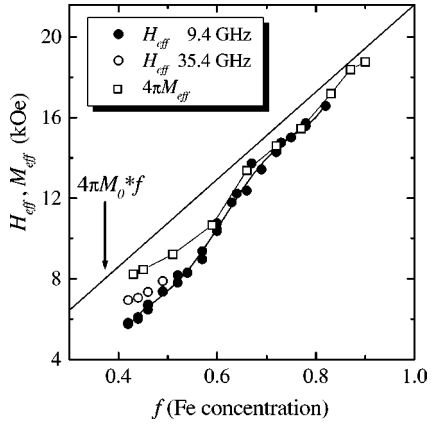

FIG. 5. Effective anisotropy fields for X ($\nu=9.4$ GHz) and Q ($\nu=35.4$ GHz) bands as a function of the Fe volume fraction. Open squares correspond to the effective magnetization expressed in Oe obtained from dc magnetization measurements. The solid line corresponds to $4\pi f M_0$ (with $4\pi M_0=21.6$ kG).

Using the experimental values of $\Delta H_{\perp}$ the parameter ε_0 can be obtained as a function of the Fe concentration. In all cases ε_0 ranges between 0.04 and 0.14 indicating that the deviation from sphere-shaped particles is small.

For parallel resonance the linewidth is assumed to come from two sources: particle shape (the resonance field is different for spheres than for ellipsoids) and particle orientation (the resonance field is larger when the ellipsoids are oriented perpendicular to the applied field). An upper estimation for the parallel linewidth is then

$$\Delta H_{\|}=H_{\|}(\varepsilon=\varepsilon_0,x=0)-H_{\|}(\varepsilon=\varepsilon_0,x=1). \tag{16}$$

With the ε_0 estimated in Eq. (15) and the parallel resonance field obtained from

$$\left(\frac{\omega}{\gamma}\right)^2=\left[H_{\|}+4\pi f M_0\left(1+(1-f)\frac{\varepsilon x}{2}\right)\right]\times\left[H_{\|}+4\pi f M_0(1-f)\varepsilon\left(x-\frac{1}{2}\right)\right], \tag{17}$$

it is possible to calculate the parallel linewidth using Eq. (16). The $\Delta H_{\|}$ values calculated from the above equations are plotted as a function of f in Fig. 4 together with the experimental values. A few values of the Q band $\Delta H_{\|}$ for the more diluted compositions are also plotted in the figure. In general the first term inside the square root in Eq. (15) is smaller than ω/γ so that $\Delta H_{\perp}\sim 4\pi f M_0(1-f)\varepsilon_0/4$. This means that to get the same ε_0 values (remember that ε_0 is only related to the microstructure), similar $\Delta H_{\perp}$ should be observed at different frequencies, and this is indeed what was found in the films that were measured in both bands. The parallel linewidth has a small dependence on ω/γ but comparable values are also expected and measured for the X and Q bands (at least for low Fe concentrations). Although the model maybe somewhat oversimplified, the estimated $\Delta H_{\|}$ are in good agreement with the measured data. Note that the only free parameter used in this description is the perpendicular linewidth and that the relatively small values obtained for the ellipticity parameter ε agree with the TEM observations of the microstructure.[5]

B. Fe concentration dependence

1. Effective anisotropy field

The coercivity obtained from magnetostatic measurements as a function of Fe concentration in a similar set of samples have shown that the Fe percolation threshold is between $f=0.62$ and $f=0.65$ in as-deposited samples.[5] With the measured resonance fields in the parallel and perpendicular directions ($H_{\|}$ and $H_{\perp}$) and using Eq. (6) it is possible to obtain the values of the effective field and the g factor as a function of the Fe volume fraction. In Fig. 5 $H_{\rm eff}=H_{\perp}+H_{\|}/2-\sqrt{(H_{\|}/2)^2+H_{\|}(H_{\|}+H_{\perp})}$ is plotted as a function of f for X band and a few low Fe concentration Q-band points. The solid line $4\pi M_0 f$ (with $4\pi M_0=21.6$ kG) represents the demagnetization term of the effective field assuming spherical particles ($\varepsilon=0$) embedded in a thin film in Eqs. (4) and (13). As mentioned before ε values are generally small, affecting the linewidth rather than the peak position. Magnetization values measured in a dc Faraday balance, are also plotted for comparison. Rubinstein[16] showed that in granular thin films the effective value of magnetization to be used in Kittel's equations [Eq. (6)] is the average or effective magnetization. This is supported by the fact that for an ideal heterogeneous composite the magnetization should vary as $M_{\rm eff}=fM_0$ identically to what it is predicted by Eq. (14) for spherical particles embedded in a thin film. The effective field can be written as

$$H_{\rm eff}=\frac{2K_z}{M_{\rm eff}}+4\pi M_{\rm eff}. \tag{18}$$

For Fe concentrations larger than 0.66 (where the network has already percolated) $H_{\rm eff}$ and $4\pi M_{\rm eff}$ have the same linear behavior with an extrapolated $4\pi M_0$ value (21 kG) slightly smaller than the accepted bulk $4\pi M_0$ value. This difference is generally attributed to the influence of surface roughness.[12] Below the percolation threshold and down to $f=0.60$ the curves are no longer linear but $H_{\rm eff}$ and $4\pi M_{\rm eff}$ are still coincident indicating that the effective anisotropy [first term in Eq. (18)] is very small. The reason for the nonlinear behavior at f_p is not clear, but may originate in the

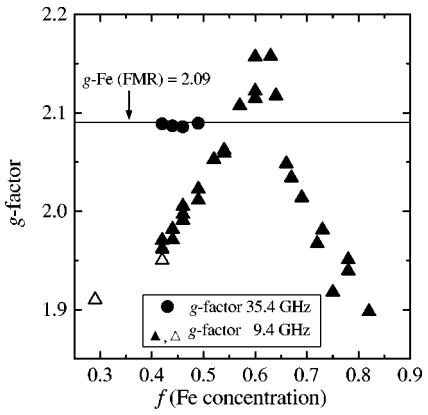

FIG. 6. g factor as a function of the Fe concentration for X ($\nu=9.4$ GHz) and Q ($\nu=35.4$ GHz) bands in as-deposited films. Open triangles are data obtained from Ref. 13. The g factor for bulk FM Fe is also indicated.

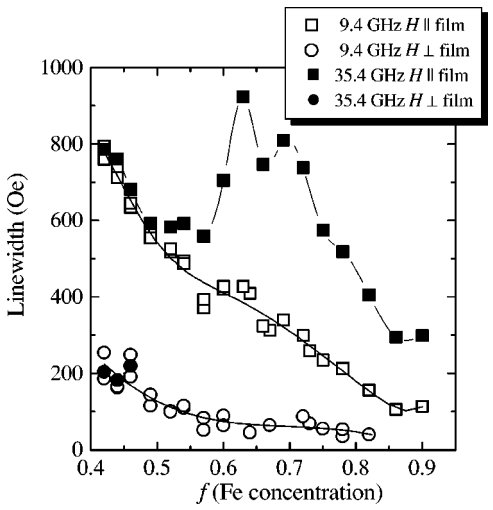

FIG. 7. Parallel and perpendicular linewidths for X ($\nu=9.4$ GHz) and Q ($\nu=35.4$ GHz) band as a function of the Fe volume fraction in as-deposited samples. Solid lines are guides to the eye.

very intricate structure of the Fe grains that are far from being spheres or a continuous plane. For lower concentrations $4\pi M_{\rm eff}$ is larger than $H_{\rm eff}$ and tends asymptotically to the $4\pi f M_0$ value again. This difference may be due to the fact that diluted samples have a larger fraction of very small nearly superparamagnetic particles so that several kOe are needed to reach saturation. In X and Q bands the perpendicular resonance field is usually larger than 10 kOe, but $H_{\parallel}$ is $\sim$1000 Oe for the X band and $\sim$7500 Oe for Q band. Measurements of the dc saturation magnetization have been made in the 10–12 kOe range. As it can be seen in the figure $H_{\rm eff}$ values obtained from the Q band are closer to $4\pi M_{\rm eff}$ and are larger than the $H_{\rm eff}$ values calculated from X-band measurements. This result supports the hypothesis of a nonsaturated magnetization in the FMR experiments. A negative effective anisotropy favoring the out-of-plane orientation of $M_{\rm eff}$ cannot be ruled out in principle [see Eq. (18)]. Resonance measurements at larger fields and frequencies are needed to elucidate this point.

2. g factor

Apart from the effective field it also possible to obtain the g factor from Eq. (6). In Fig. 6 the values obtained from X-band measurements are plotted as a function of f. It can be seen that the g factor is concentration dependent and peaks at the percolation concentration. Two extra g values in the diluted Fe region, obtained from Ref. 13,[20] are consistent with our own data. In general the values of g are lower than the expected value for thin Fe films ($g=2.09$). The analysis of the g factors obtained from the X band must be made with care. The fact that the magnetization is not fully saturated for the parallel resonance measurements when $f<0.6$ can affect the results. For example, in the $f=0.42$ sample a value of $g=2.10$ can be obtained if $M=0.82M_0$ is assumed for parallel resonance and $M=M_0$ for perpendicular resonance. The g factors for diluted samples obtained from Q-band measurements are all very close to 2.09, supporting the fact that the X-band values may be influenced by the nonsaturation of M. Unfortunately the maximum available field was not large enough to allow out-of-plane Q-band measurements for higher Fe concentrations. The decrease in g observed for $f>0.6$ should not originate, in principle, in superparamagnetic effects ($H_{\rm eff}\approx 4\pi M_{\rm eff}$ as can be seen in Fig. 5). If the slope of the hysteresis loop does not change significantly for large Fe concentrations and because $H_{\parallel}$ is smaller for larger f, the resonance may be taking place in a region of the loop where $M<M_{sat}$ giving a smaller g. This suggestion needs to be confirmed with a careful comparison between $M-H$ loops and resonance data.

3. Linewidth

The resonance linewidth was also measured as a function of the Fe content. X- and Q-band values for H applied parallel and perpendicular to the film are plotted in Fig. 7. Due to field limitation only a few Q-band $\Delta H_{\perp}$ points could be measured. As discussed in Sec. III A 2 the experimental linewidth can be thought of as the sum of a very large number of lines with an intrinsic narrow linewidth resonating at different fields. The intrinsic relaxation is given by Eqs. (7) and (8) and the variation in the resonance fields was assumed to come from a distribution of particle shapes and orientations [Eqs. (15) and (16)]. The concentration dependence in Eq. (7) comes from the $1/M_0$ term that, as explained in Ref. 16, should be replaced by $1/fM_0$. Thus for both parallel and perpendicular linewidths we have

$$\Delta H_{\parallel}=\Delta H_{\perp}\approx \frac{2\lambda}{\gamma f M_0}\,\frac{\omega}{\gamma} \quad (\Delta\theta\sim 0). \tag{19}$$

In the case of line broadening by shape and orientation effects it is possible to obtain the following approximate expressions:

$$\Delta H_{\perp}\approx 4\pi f M_0(1-f)\,\frac{\varepsilon_0}{4}, \tag{20a}$$

$$\Delta H_{\parallel}\approx \Delta H_{\perp}\left(3+\frac{4\pi f M_0}{\sqrt{(4\pi f M_0)^2+(\omega/\gamma)^2}}\right)\approx 4\Delta H_{\perp}. \tag{20b}$$

Two important differences exist between the mechanisms described above. The LL relaxation predicts similar linewidths that increase with frequency. The shape-orientation model predicts $\Delta H_{\parallel} \approx 4\Delta H_{\perp}$ and no frequency dependence. Both models give a decreasing linewidth for increasing Fe volume fraction. The experimental results shown in Fig. 7 can be explained if two different regions are distinguished. For low Fe concentrations and up to $f \sim 0.5$, *X*- and *Q*-band results are coincident with $\Delta H_{\parallel}/\Delta H_{\perp} \approx 4$. This fact strongly indicates that the intrinsic linewidth is small and that the major broadening mechanism is due to shape-orientation. For $f > 0.5$ a frequency dependence appears for $\Delta H_{\parallel}$. The *Q*-band linewidth even peaks near f_p while a small bump is observed for the *X*-band $\Delta H_{\parallel}$. The maximum in $\Delta H_{\parallel}$ can be attributed to a sudden increase of λ occurring at this concentration. A peak in the intrinsic relaxation of granular composites has been previously observed[12] and was related to the maximum in the correlation length (which describes the size of finite clusters) occurring at the percolation threshold.

4. Sample annealing

The purpose of sample annealing is to study the influence of changing the particle size and shape on the magnetic properties. After annealing, the particle size and the distribution of sizes normally increases. The particle shape tends to be more spherical (constrained by the film thickness) also with a larger distribution.[5] We have found that the effective anisotropy field remained almost unchanged after annealing. This is an indication that the effective demagnetization factor did not change significantly. The linewidth increased by a factor ~ 6 in the out-of-plane orientation and a factor $\sim 2-4$ in the in-plane direction. The overall increase in the linewidth indicates that the distribution of particle shapes is much larger in the annealed state. However, the ratio $\Delta H_{\parallel}/\Delta H_{\perp}$ diminished to a factor ~ 2 suggesting that, as expected, the particles are more isotropic in the film plane.

5. In-plane anisotropy

As mentioned in Ref. 5 Fe-rich samples ($f \gtrsim 0.7$) present a uniaxial anisotropy with the easy axis parallel to the direction of the composition gradient. From magnetization measurements it was found that the coercive field parallel to the easy axis has almost the same value as the anisotropy field (~ 30 Oe), indicating that the Fe grains are single domain. Up to now it was assumed that there was no anisotropy in the film plane. To take into account the presence of in-plane anisotropy the equation for parallel resonance [Eq. (6b)] has to be modified in the following way:[14]

$$\left(\frac{\omega}{\gamma}\right)^2 = (H - H_A)(H + H_{\text{eff}}) \quad \alpha = \pi/2, \varphi = \pi/2 \quad (H > H_A), \tag{21a}$$

$$\left(\frac{\omega}{\gamma}\right)^2 = (H + H_A)(H + H_A + H_{\text{eff}}) \quad \alpha = \pi/2, \varphi = 0, \tag{21b}$$

where H_A is the in-plane anisotropy field representing an easy axis parallel to the composition gradient. In general $H_{\text{eff}} \gg H$, H_A for the *X* band so that the second term in parenthesis in the above equations can be replaced by H_{eff}.

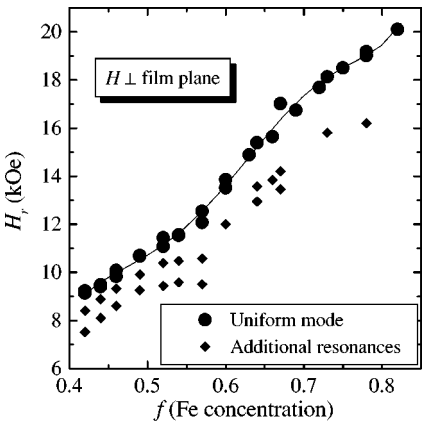

FIG. 8. Uniform mode and additional resonance lines observed in as-deposited samples for *H* applied perpendicular to the film plane as a function of *f* [*X*-band ($\nu = 9.4$ GHz) measurements]. The solid line serves as a guide to the eye.

With this approximation the in-plane anisotropy field can be written as $H_A = (H_{\perp} - H_{\parallel})/2$. Using the resonance fields $H_{\perp} = 682.5$ Oe and $H_{\parallel} = 630.5$ Oe measured for the $f = 0.9$ film, $H_A = 26$ Oe is obtained, totally consistent with magnetization measurements. The very small value of H_A compared to H_{eff} justifies the noninclusion of an in-plane anisotropy term in Eq. (1). The origin of this small anisotropy is believed to come from a very small elongation of the magnetic particles in the direction of the composition gradient due to the geometry of the sputtering process.

C. Additional resonances

When the external field is applied perpendicular to the film plane it is possible to observe one or two weak additional resonances at fields lower than the main resonance absorption corresponding to the uniform precession mode. When $f < f_p$ two extra lines are always observed, while for $f > f_p$ one or two lines may be found (see Fig. 8). The average separation between the additional lines is $\sim 800 \pm 140$ Oe. The separation between the center of gravity of the extra absorptions and the principal line tends to increase with increasing concentration. These extra modes do not appear to be standing spin waves because the separation between consecutive modes decreases instead of increasing. It is possible that the peculiar microstructure of the films is the source of these extra resonances that could be eigenmodes or even magnetostatic modes. None of these extra lines are seen after annealing.

Additional resonances of another type can be observed *only* for Fe concentrations very close to the percolation threshold. These lines are equally spaced and have been observed for $f = 0.63$, 0.66, and 0.69 only in as-deposited samples. They are also very sensitive to the exact perpendicular alignment between the film and the external field. Moving *H* 3 degrees out of the film normal causes all lines to disappear. The largest number of lines was found for $f = 0.66$: 16 lines with an average field separation of 55 ± 12 Oe. The line position relative to the first mode is plotted in Fig. 9. Data for this film and the other two compositions are presented in Table I. It is interesting to note that the minimum field separation occurs for the composition where

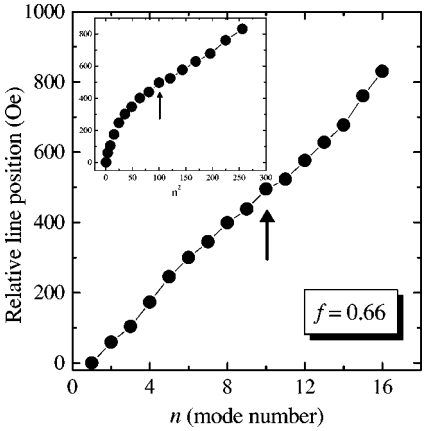

FIG. 9. Additional resonance absorptions associated to standing spin waves observed for H applied perpendicular to the film plane. The line position is plotted relative to the first mode. X-band ($\nu = 9.4$ GHz) data for $f = 0.66$ are presented. The inset shows the same data plotted as a function of n^2. The transition from linear to parabolic behavior occurs around $n' \sim 10$.

the maximum number of lines is observed. In general, the field separation and the intensity of the peaks depend on the spin pinning, magnetic anisotropy, sample homogeneity, etc. One simple case consists of assuming that (a) spins are pinned to the surface, (b) the internal static field and the oscillatory field are homogeneous inside the sample, (c) the magnetization is saturated and the anisotropy within the film is zero. Under these assumptions Eq. (6a) takes the form[21]

$$\frac{\omega}{\gamma} = H - H_{\text{eff}} + \frac{D}{g\mu_\beta} k^2. \tag{22}$$

The parameter D is termed the exchange constant. The wave vector k is defined as $k = n\pi/L$, with n the mode number (that can only be odd because of symmetry considerations) and L is the wavelength of the standing spin wave (usually equals the film thickness in homogeneous thin films). See that Eq. (22) predicts a line position proportional to n^2 and a linear separation between consecutive lines,

$$\Delta H_n = 4(n+1)\frac{D}{g\mu_\beta}\left(\frac{\pi}{L}\right)^2 \quad (n \text{ odd}). \tag{23}$$

In order to explain the tendency towards a linear mode separation for low n, a parabolic variation of the magnetization through the film thickness was assumed [i.e., $M(z) = M(1 - 4\sigma z^2/L^2]$, together with no surface pinning.[22] This model, known as the volume inhomogeneity model, predicts a constant separation between consecutive lines: $\Delta H_n = 8\sqrt{4\pi M_0 \sigma D/g\mu_\beta}/L$, and a transition from linear to quadratic behavior for the mode n' satisfying

$$n' = \frac{1}{2}\left(L\sqrt{\pi M_0 \sigma \Big/ \frac{D}{g\mu_\beta}} - 1\right)$$
$$\approx \frac{1}{2}\left(\frac{L^2 \Delta H_{n'}}{16 D/g\mu_\beta} - 1\right) \Rightarrow \Delta H_{n'}$$
$$\approx (2n'+1)\frac{16D}{L^2 g\mu_\beta}. \tag{24}$$

The accepted value[23] for the exchange constant D in Fe films at room temperature is $D = 5\times10^{-29}$ erg cm^2. For granular Fe-SiO_2 films Chien[24] have found that the magnetization follows $M(T) = M_0(1 - BT^{3/2})$, temperature dependence indicating the presence of spin-wave excitations. He deduced a spin-wave constant B much larger than the value for bulk Fe. The constant B is related to the exchange constant D by[25] $M_0 B = g\mu_\beta \zeta(3/2)(k_B/4\pi D)^{3/2}$ (ζ is Riemann zeta function, k_B is the Boltzmann constant). From the B value given in Ref. 24 it is possible to obtain $D = 8.3\times10^{-30}$ erg cm^2. Chien suggested several possibilities for a D value smaller than the bulk counterpart, among them the abundance of magnetic surfaces, a modification of the spin-wave spectrum, or a cut off of the spin waves with wavelengths larger then the physical dimensions of the particles.

From Eq. (23) it can be seen that standing spin waves could hardly be observed in continuous thin films thinner than ~ 100 nm because of the very large separation between modes. Even with the smaller D value found in granular Fe films a field separation of ~ 7500 Oe is estimated for 20 nm films, more than two orders of magnitude larger than the actual value. In Ref. 13 a set of equally spaced (174 Oe) lines was also observed in thick (~ 400 nm) Fe-SiO_2 films. It was suggested that the wavelength of the standing spin wave was related to the film thickness rather than to the size of the Fe granules. However, our measurements in thinner films show that the line spacing not only does not increase as expected if L was equal to the film thickness, but decreases to ~ 55–85 Oe. This strongly indicates that the wavelength is related to another physical length. The fact that these lines are only observed very close to the percolation threshold suggests that there may be a connection between L and the correlation length ξ (that is a measure of the size of the connected regions or granules). The correlation length normally increases as f is increased, diverging at f_p where an infinite cluster is formed. Above f_p the infinite cluster grows at the expense of finite clusters and ξ decreases. Because of the linear mode separation it is more appropriate to use Eq. (24) to calculate the characteristic length. For $f = 0.66$ a linear to parabolic transition occurs for $n' \sim 10$ (see the inset of Fig. 9) For the other two concentrations no transitions could be observed due to the small number of lines and n' was chosen to be equal to the total number of lines. The estimated values of L are also reported in Table I. It is interesting to note that the characteristic length has a maximum at the intermediate concentration, coincident with what would be expected for the correlation length. Although this coincidence may be fortuitous since none of the spin-wave models

TABLE I. Number of lines observed, average line separation, transition from linear to parabolic behavior, and characteristic length for the three Fe concentrations where additional resonances were detected. To calculate L we used $D = 8.3\times10^{-30}$ erg cm^2 deduced from the B value given in Ref. 24.

f	Number of lines	Average separation	n'	L (nm)
0.63	6	65 ± 8	6	370
0.66	16	55 ± 12	10	511
0.69	4	84 ± 11	4	271

is completely adequate to describe an heterogeneous thin film, it seems clear that the wave length of the standing spin waves is not strictly related to the film thickness in these materials.

IV. CONCLUSIONS

A ferromagnetic resonance investigation of a series of Fe-SiO_2 thin films has shown that the size, shape, and shape distribution of the Fe granules play a major role in the observed magnetic properties. All the measured parameters $(H_{\rm eff}, \Delta H, M_{\rm eff}, g)$ have distinctive features at the percolation threshold of the Fe grains occurring for $f \sim 0.62$. When f is very close to f_p a large number of equally spaced lines is detected. From the line separation it is concluded that there is no relation between L and the film thickness. The wavelength seems to be related to the correlation length. Additional measurements for different thicknesses are needed to corroborate this hypothesis.

ACKNOWLEDGMENTS

We wish to acknowledge the support of Fundación Antorchas, Argentina, NSF-DMR-9713497, and the use of facilities supported by NSF-DMR-9809423. Thanks are due to Dr. Jianhua Du for helpful TEM micrographs.

*Also at Consejo Nacional de Investigaciones Científicas y Técnicas, Argentina. Electronic address: butera@cab.cnea.gov.ar

[1] A.E. Berkowitz, J.R. Mitchell, M.J. Carey, A.P. Young, S. Zhang, F.E. Spada, F.T. Parker, A. Hutten, and G. Thomas, Phys. Rev. Lett. **68**, 3745 (1992); J.Q. Xiao, J.S. Jiang, and C.L. Chien, *ibid.* **68**, 3749 (1992)

[2] S.H. Liou and C.L. Chien, Appl. Phys. Lett. **52**, 512 (1988).

[3] C.L. Chien, Annu. Rev. Mater. Sci. **25**, 129 (1995), and references therein.

[4] G. Xiao and C.L. Chien, Appl. Phys. Lett. **51**, 1280 (1987).

[5] J.N. Zhou, A. Butera, H. Jiang, and J.A. Barnard, J. Appl. Phys. **84**, 5693 (1998); J.N. Zhou, A. Butera, H. Jiang, D.H. Yang, and J.A. Barnard, *ibid.* **85**, 6151 (1999).

[6] H. Hurdequint, J. Magn. Magn. Mater. **93**, 336 (1991).

[7] M.J. Hurben, D.R. Franklin, and C.E. Patton, J. Appl. Phys. **81**, 7458 (1997).

[8] S. Chikazumi, *Physics of Magnetism* (Krieger, Melbourne, FL, 1978), p. 51.

[9] C. Kittel, *Introduction to Solid State Theory*, 7th ed. (Wiley, New York, 1996), p. 506.

[10] K.B. Urquhart, B. Heinrich, J.F. Cochran, A.S. Arrott, and K. Myrtle, J. Appl. Phys. **64**, 5334 (1988).

[11] D.L. Griscom, J.J. Krebs, A. Perez, and M. Treilleux, Nucl. Instrum. Methods Phys. Res. B **32**, 272 (1988).

[12] R.L. Holtz, P. Lubitz, and A.S. Edelstein, Appl. Phys. Lett. **56**, 943 (1990).

[13] W.N. Wang, Z.S. Jiang, and Y.W. Du, J. Appl. Phys. **78**, 6679 (1995).

[14] C. Vittoria, *Microwave Properties of Magnetic Films* (World Scientific, Singapore, 1993), Chap. V.

[15] U. Netzelmann, J. Appl. Phys. **68**, 1800 (1990).

[16] M. Rubinstein, B.N. Das, N.C. Koon, B.D. Chrisey, and J. Horwitz, Phys. Rev. B **50**, 184 (1994); M. Rubinstein, J. Tejada, and X.X. Zhang, J. Appl. Phys. **75**, 6557 (1994).

[17] C. Kittel, Phys. Rev. **73**, 155 (1948).

[18] V. Siruguri and S.N. Kaul, J. Phys.: Condens. Matter **8**, 4567 (1996).

[19] J. Dubowick, Phys. Rev. B **54**, 1088 (1996).

[20] The authors in Ref. 13 did not calculate the g factor, but used instead the value mentioned in Ref. 12 ($g = 2.02$). However, from their experimental $H_{\parallel}$, $H_{\perp}$, and $\omega/2\pi$ data it is possible to obtain the g factors plotted in Fig. 6.

[21] T.G. Phillips, Proc. R. Soc. London, Ser. A **292**, 224 (1966).

[22] A.M. Portis, Appl. Phys. Lett. **2**, 69 (1963).

[23] T.G. Phillips, Phys. Lett. **17**, 11 (1965); S.A. Oliver, C. Vittoria, E. Schloemann, H.J. Van Hook, and R.W. Tustison, J. Appl. Phys. **63**, 3802 (1988).

[24] C.L. Chien, J. Appl. Phys. **69**, 5267 (1991).

[25] T.G. Phillips and H.M. Rosemberg, Rep. Prog. Phys. **29**, 285 (1966).